ELSEVIER

Polymer 41 (2000) 595–606

polymer

Copolymerization of 1,2 bis(2-methylpropenoyloxy)ethane and divinylbenzene in aqueous suspension. Part I: control of the diameters of the beads of 1,2 bis(2-methylpropenoyloxy)ethane–divinylbenzene copolymer

C. Gaillard[a], M. Camps[a,*], J.P. Proust[b], I.A. Hashieh[b], P. Rolland[b], A. Bois[c]

[a]*Laboratoire de Chimie des Macromolécules, Université de Provence, 3 place Victor Hugo, 13331 Marseille, France*
[b]*Laboratoire d'odontologie IMEB, 27 Bd J. Moulin, 13385 Marseille, France*
[c]*Laboratoire d'Optoélectronique, Université de Toulon, Ifremer-Université, BP 330, 83506 La Seyne sur Mer, France*

Received 9 June 1998; received in revised form 14 February 1999; accepted 12 March 1999

Abstract

The aim of the current paper is to study the influence of the interfacial tension (σ) and viscosity on the droplets dispersion of 1,2 bis(2-methylpropenoyloxy)ethane (EGDMA) and divinylbenzene (DVB). This dispersion is characterized by the distribution of poly(EGDMA-coDVB) polymer spheres. We experimentally observed that this distribution is polymodal and that the experimental maximum diameter $(d_{max})_{obs}$ is proportional to $(\sigma/\rho_c)^{0.59}$ (ρ_c is the continuous phase density). This relation is valid when $(d_{max})_{obs} \gg \eta$, the Kolmogoroff turbulence microscale (which is related to the dissipated power by mass unit and the kinematic viscosity (ν_c) of the continuous phase). When $(d_{max})_{obs} \ll \eta$, the experimental maximum diameter is not proportional to $(\nu_c\sigma/\rho_c)^{1/3}$, but it verifies the theory of Taylor's viscous shear abrasion where the maximum diameter is proportional to $\sigma/[\mu_c(19p + 16)/(16p + 16)]$ ($p = \mu_d/\mu_c$, μ_d and μ_c are the dynamic viscosity of the dispersed and continuous phase, respectively).

Keywords: Poly(1,2 bis(2-methylpropenoyloxy)ethane-co-divinylbenzene); Liquid–liquid dispersion; Polymerization suspension

1. Introduction

1,2 bis(2-methylpropenoyloxy)ethane is usually referred to as ethylene glycol dimethacrylate (EGDMA) which will be used throughout in this work. EGDMA is associated in minor quantities with monomers such as styrene [1], hydroxyethylmethacrylate [2], acrylic acid [3], etc. and it is often used as a reticulating agent. Few studies have been conducted on the copolymerization in suspension of EGDMA. Yang and Hamann [1] measured the conversion of the mixture of EGDMA-DVB (DVB: divinylbenzene). Sakado and Kida [4] claimed the preparation of "microsponge" from a mixture of EGDMA and methylmethacrylate.

Our aim is to establish the relations giving the maximum bead diameter as a function of the interfacial tension and the viscosity for a particular reactor and stirrer without a baffle.

The polymerization in suspension is a procedure which is based on the dispersion of a organic phase composed of at least one monomer and an initiator in a liquid which does not solubilize any of the components of the organic phase. In most cases, water is used to achieve the dispersion [5]. Each droplet constitutes a homogenous radical micropolymerization [6] and yields a polymer bead.

The main difficulty in the preparation of the polymer beads is the control of their mean diameter. This is also one of the mean diameter of the droplets at the time of polymerization in an unstable liquid–liquid suspension kept in this state by mechanical stirring. In this type of dispersion, the droplets diameters depend on multiple parameters such as the stirring speed, the interfacial tension, the viscosity of the phases, the presence of a protective colloid, etc.

The mean diameter prediction must take into account complex breaking and coalescing phenomena which are difficult when related to the theoretical bases. In contrast, there are established theoretical relationships between the maximum diameter of a droplets distribution and different experimental parameters. The mean diameter can be determined from the maximum diameter by way of the experimental proportional relationship between the mean and maximum diameters [7].

* Corresponding author.

0032-3861/00/$ - see front matter
PII: S0032-3861(99)00207-4

Nomenclature

C_P	heat capacity (J kg^{-1} K^{-1})
D	stirrer anchor-shaped circle arc diameter (m)
D_T	reactor diameter (m)
d	theoretical droplet diameter in mathematical developments (m)
d_{obs}	experimental droplet diameter (m)
d_{32}	Sauter mean diameter (m)
$\bar{d}$	mean diameters of droplets (m)
d_{max}	theoretical maximum diameters (m)
$(d_{max})_{obs}$	experimental maximum diameter (m)
$\bar{d}^{nb}$	number mean diameter (m)
$\bar{d}^{w}$	weight mean diameter (m)
e	stirrer width (m)
$E(k)$	energy distribution (J kg^{-1}) for a wave number k (m^{-1})
f_c	circulation speed or frequency (s^{-1})
$f(p)$	dimensionless viscosity function $(19p + 16)/(16p + 16)$
G	velocity gradient or abrasion velocity (s^{-1})
k	wave number k (m^{-1})
l	length of the stirrer anchor-shaped circle arc (m)
N	stirring speed (s^{-1})
N_{vi}	dispersed phase viscosity number (dimensionless)
p	viscosity ratio $= \mu_d/\mu_c$ (dimensionless)
P	dissipated power (W)
ΔP_G	pressure difference established in the drop/surrounding liquid interface (Pa)
Re	Reynolds number (dimensionless)
Re_T	apparatus Reynolds number (dimensionless)
S	droplet surface (m^2)
Ta	Taylor number (dimensionless)
u	flow velocity (m s^{-1})
V_c	continuous phase (aqueous solution of acacia gum and surfactant) volume (m^3)
V_d	dispersed phase (organic phase) volume (m^3)
$\vec{V}$	velocity vector (m s^{-1})
We	Weber number (dimensionless)
We_{crit}	critical Weber number (dimensionless)
We_T	Weber number of the apparatus (dimensionless)
ε	dissipated power by mass unit (W kg^{-1})
η	turbulence microscale value of Kolmogoroff, $\eta = \varepsilon^{-1/4}\nu_c^{3/4}$ (m)
$\Delta\theta$	temperature increase (K)
μ_c	dynamic viscosity of continuous phase (Poiseuille–Pl)
μ_d	dynamic viscosity of dispersed phase (Pl)
ν_c	kinematic viscosity of the continuous phase (m^2 s^{-1})
ρ_c	density of continuous phase (kg m^{-3})
ρ_d	density of dispersed phase (kg m^{-3})
σ	interfacial tension between the dispersed and continuous phase (N m^{-1})
φ	phase volume fraction (dimensionless)
ϑ	angle formed by the major axis of a deformed drop with a perpendicular to the velocity vector (rad)
$\Psi(N_{vi})$	function of the dispersed phase viscosity number (dimensionless)

Subscripts

c	continuous phase (aqueous solution of acacia gum and surfactant)
d	dispersed phase (organic solution)

Since few theoretical data justify the methods referenced to in the literature for the industrial preparation of main polymers such as poly(vinylchloride) [8], poly(acrylonitrile) [9] under the form of beads, it was necessary to examine the theoretical bases of liquid–liquid dispersion.

In Section 2, we discuss the main theoretical relations which describe the division state of the droplets diameter's distribution.

2. Theoretical part

2.1. Droplets theoretical maximum diameters of liquid–liquid suspension according to the inertial breakup theory of Kolmogoroff valid for a turbulent flow

The stirring of liquid–liquid suspensions produces, from a hydrodynamic point of view, a very complex turbulent flow. This flow depends mainly on the Reynolds number (Re), a dimensionless number, which is the ratio of inertial forces to viscous forces [10]:

$$\mathrm{Re} = \frac{Lu}{\nu_c}, \tag{1}$$

where L is a length, u the flow velocity and ν_c the kinematic viscosity.

For a given flow, Re has several relations which depend on the observing scale of the flow phenomenon. In a turbulent flow, large eddies produce smaller ones which themselves produce even smaller ones… The smallest eddies do dissipate the energy as heat. Below a certain size the eddies depend no more on the turbulent flow macroscopic characteristics. The size of a given eddy is the distance necessary for a full rotation (see Fig. 1).

Kolmogoroff [11] suggested the hypothesis that there is a turbulence domain where the turbulent field is homogenous and isotropic.

At this scale, the probability laws do not depend anymore on the turbulent flow macroscopic characteristics, but depends on d, ε and ν_c (d stands for the phenomenon scale, ε the dissipated power by mass unit and ν_c the liquid kinematic viscosity of the continuous phase). A turbulence is homogenous and isotopic when its statistical properties are invariant by translation, rotation and reflection of the coordinates system [12].

The dispersed droplets are very small compared to large scale eddies which can be assimilated to the stirrer blade

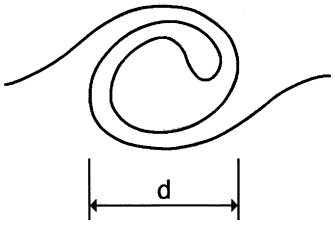

Fig. 1. Eddy of wavelength d.

diameter D. This implies that at the droplet scale the turbulence is locally isotropic and homogenous. Thus, the probability laws depend only on ε, ν_c and d (d stands for the droplet diameter). In order to attribute kinematic energies for each droplet size it is necessary to formulate the energy exchanges in the Fourier's space where each wavelength is associated to a wave number k [13]:

$$k = \frac{2\pi}{d}. \tag{2}$$

The theoretical developments [12,13] allows to obtain the following energy distribution $E(k)$ in function of ε, ν_c and k according to the first hypothesis of Kolmogoroff [11,12]:

$$E(k) = \varepsilon^{1/4}\nu_c^{5/2}F(k\eta), \tag{3}$$

where

$$\eta = \varepsilon^{-1/4}\nu_c^{3/4}. \tag{4}$$

Since η and k have length and inverse length as dimension unit, respectively, F is a function of the dimensionless product $k\eta$

$$E(k) \propto \varepsilon^{1/4}\nu_c^{5/2}. \tag{5}$$

Relation which is valid for:

$$D \gg \eta \gg d. \tag{6}$$

According to the second hypothesis formulated by Kolmogoroff [11,12], there is a turbulence domain where the probability laws depend only on ε and d only without the intervention of the viscosity.

In this domain

$$D \gg d \gg \eta. \tag{7}$$

In this case

$$E(k) \propto \varepsilon^{2/3}k^{-5/3}. \tag{8}$$

In a turbulent flow, inertial, viscous and internal energy forces interact on a liquid droplet of size d and energy $E(k)$. The internal energy is σS, where σ is the interfacial tension and S is the droplet surface [14]. The maximum stable diameter is determined by the ratio between the internal cohesion forces and the inertial and viscous forces [15]

$$\sigma S = m\int_{k_{\max}}^{\infty} E(k)\,\mathrm{d}k, \tag{9}$$

where m is the droplet mass.

In the case where $D \gg d \gg \eta$, we obtain (see Appendix A):

$$d_{\max} \propto \left(\frac{\sigma}{\rho_c}\right)^{3/5}\varepsilon^{-2/5} \tag{10}$$

where ρ_c is the density of continuous phase.

In the case where $D \gg \eta \gg d$, we obtain (see Appendix

A):

$$d_{\max} \propto \left(\frac{\nu_c \sigma}{\varepsilon \rho_c}\right)^{1/3}. \quad (11)$$

These relationships may be obtained by way of the Weber number (see Appendix A). Parameters σ and ν_c may be easily modified by the addition of a surfactant or a viscous substance, ε depends on the stirring power and can be calculated.

2.2. Droplets theoretical maximum diameters of liquid–liquid suspension according to the viscous shear breakup theory of Taylor

Taylor [16–18] showed that the droplets in a viscous abrasion field are sheared when the pressure difference ΔP_G (established at the interface between the drop and the surrounding liquid) is greater than the internal cohesion forces.

Thus

$$\Delta P_G > 2\sigma/d. \quad (12)$$

In a laminar flow, Taylor [16–18] theoretically and experimentally established that ΔP_G follows the relation:

$$\Delta P_G = -4G\mu_c\left[\frac{19p+16}{16p+16}\right]\sin 2\varphi, \quad (13)$$

where G is the velocity gradient or abrasion velocity (expressed in s^{-1}), $p = \mu_d/\mu_c$, μ_d is the discontinuous phase (organic phase) viscosity, μ_c the continuous phase (aqueous phase) viscosity and φ the angle formed by the major axis of a deformed drop with a perpendicular to the velocity vector ($\bar{V}$) (Fig. 2).

Combining relations (12) and (13), and assuming that $\sin 2\varphi \sim 1$, $d_{\max}$ can be expressed as [19]:

$$d_{\max} = \frac{\sigma}{2G\mu_c\left[\frac{19p+16}{16p+16}\right]} \quad (14)$$

.

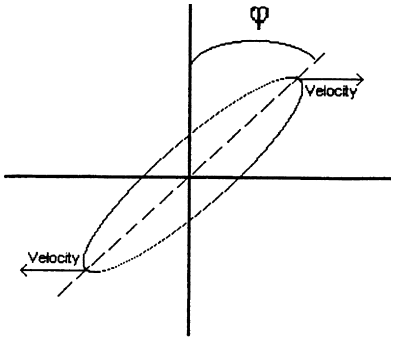

Fig. 2. Angle φ formed by the axis of deformed drop with a perpendicular to the velocity vector $\bar{V}$.

3. Experimental

3.1. Definition of mean diameters $\bar{d}$, number and weight fractions X_i of droplets

Number mean diameter $\bar{d}^{nb}$, weight mean diameter $\bar{d}^{w}$ and Sauter mean diameter d_{32}:

$$\bar{d}^{nb} = \sum_1^n X_i^{nb} d_i, \quad (15)$$

$$\bar{d}^{w} = \sum_1^n X_i^{w} d_i, \quad (16)$$

$$d_{32} = \frac{\sum_1^n X_i^{nb} d_i^3}{\sum_1^n X_i^{w} d_i^2}. \quad (17)$$

Number and weight fractions:

$$X_i^{nb} = \frac{n_i}{n}, \quad (18)$$

where n_i is the number of droplets of diameter d_i for a sample of n droplets

$$X_i^{w} = \frac{m_i}{m}, \quad (19)$$

m_i is the weight of droplets of diameter d_i, m is the weight of sample

$$m = \sum m_i, \quad (20)$$

$$m_i = (n_i \rho \pi d_i^3)/6. \quad (21)$$

Thus, Eq. (16) can also be expressed as:

$$\bar{d}^{w} = \frac{\sum_1^n n_i d_i^4}{\sum_1^n n_i d_i^3}. \quad (22)$$

The general equation for the average diameters is [7]:

$$\bar{d}_{pq} = \frac{\sum_1^n n_i d_i^p}{\sum_1^n n_i d_i^q}, \quad (23)$$

where $p - q = 1$; p and q are positive integers.

3.2. Materials

Divinylbenzene (DVB) is a commercial mixture containing meta and para isomers (55%) and ethylbenzene, 98% purity EGDMA were purchased from Aldrich Chemical. These products were distilled under reduced pressure before use. Toluene (free of CS_2) from Aldrich Chemical was

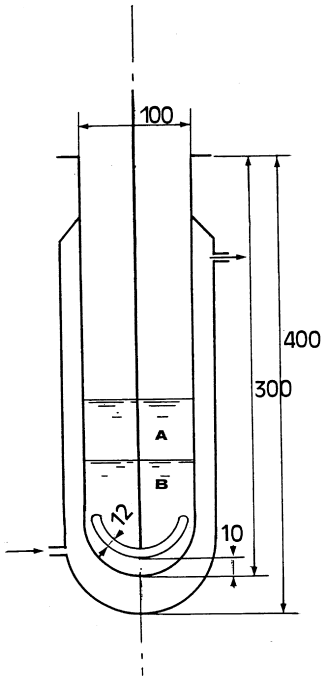

Fig. 3. Schematic representation of apparatus and disposition of the phases A and B (before stirring). All of the dimensions are stated in millimeter.

distilled. Benzoyl peroxide (BPO) with 30% of water was dissolved in chloroform then precipitated with methanol and dried under reduced pressure at room temperature. Acacia gum and sodium dodecylsulfate from Aldrich were used without further purification. All of the aqueous solutions were prepared with permuted water.

3.2.1. Macroscopic homogeneity of the stirring

Fig. 3 depicts the reactor used to prepare the beads. Its capacity is 3 l. In the reactor two regions can be distinguished: one close to the stirrer extremity and the other one distant from the stirrer. For many authors, the absence of macroscopic homogeneity accounts for the heterogeneous droplet distributions even though the flow is locally homogenous and isotropic, as it is seen under the theoretical concept concerning the droplets diameters. The absence of a macroscopic homogeneity of the flow leads to a slowing down of the stirring. The fluid circulation speed or frequency f_c expressed in s^{-1}, is different from the stirring speed N (in s^{-1}) [20]:

$$\frac{f_c}{N} = \frac{1}{0.85}\left(\frac{D}{D_T}\right)^2, \tag{24}$$

where D is the stirrer length and D_T the reactor diameter.

As there is a small difference (0.01 m) between D and D_T, for $N = 5.5\ s^{-1}$ we have $f_c = 5.24\ s^{-1}$. Thus we can conclude that there is no stirring slowdown in our reactor.

3.2.2. Beads preparation

Later the organic phase is equally called dispersed phase and the aqueous solution of acacia gum and sodium dodecylsulfate is equally called continuous phase. In this work, for each trial, the dissipated power was maintained constant by fixing the rotation speed. Three series of experiments were carried out: series A (A/4 to 4A), series C_E (C_E/4 to 4C_E) and series C_A (C_A/4 to 36C_A). In these experiments, the organic phase composition was kept constant (see Table 1). In the experiments conducted on series A, the aqueous and organic phases composition was kept constant and only the volume ratio between both phases varied (see Table 1). In series C_E and series C_A the volume ratio between the phases was kept constant.

In series C_E the only parameter that varied was the surfactant concentration while in series C_A, the only parameter which varied was the acacia gum concentration (see Table 1).

3.2.3. Typical procedure

Experiment C_A: The polymer beads are prepared in the reactor shown in Fig. 3, by adding 37 ml of the organic phase and 86 ml of the aqueous phase. The organic phase is made up of 15 g EGDMA, 1.37 g divinylbenzene, 0.112 g benzoyl peroxide and 20 ml toluene. The aqueous phase is prepared as follows: 1.70 g of acacia gum are dissolved into 50 ml water, this solution is immediately filtered through hydrophylic cotton to eliminate bark particle. Later, 0.0225 g sodium dodecylsulfate are added and the aqueous phase volume is adjusted to 86 ml. The stirring is kept constant at 5.5 revolutions/s. Temperature was kept at 78 ± 1°C. As long as the temperature and the composition of organic phase were kept constant, the gelation time was also constant. From several measurements this time was calculated to be 20 ± 3 min. The gel time was previously determined by bubbling nitrogen through the organic phase (the gelation is achieved when the bubbles cannot escape anymore from the organic phase).

After 30 min (gel time + 5 min), a volume of 2.5 l of the continuous phase is added to avoid the beads agglutination, this volume does not have any effect on the beads diameter since they are already formed after the gelation time. The polymerization process is followed for about 4 h then the temperature is allowed to decrease and the mixture is kept under stirring for 17 h at 2 revolutions/s. The beads were rinsed with water and purified by soxhlet extraction for 10 cycles for 8 h using methanol as solvent. The beads were then vacuum dried (0.1 mmHg and 65°C) for 6 h. The beads with a diameter greater than 45 μm were separated by sieving. The liquid containing the smaller beads was then decanted. The supernatant was removed suction.

3.2.4. Aqueous solutions viscosity

It was measured with an Ubbehlod viscometer (0.5 mm capillary) at 78 ± 0.1°C.

3.2.5. Interfacial tension

The pendant drop tensiometer is based on an integrated form of the Laplace equation for a drop interface, in which

Table 1
Composition of organic and aqueous phases

Series	Organic phase					Aqueous phase					
	EGDMA[a] (g)	DVB[a] (g)	Toluene (ml)	BPO[a] (g)	V_{org}[b] (ml)	Water (ml)	AG[a] (g)	SDS[a] (g)	V_{aq}[b] (ml)	V_{total}[b] (ml)	ϕ[a]
A/4	3.75	0.35	5	0.028	9.5	86	1.70	0.0225	86	95.5	0.099
A/2	7.50	0.69	10	0.056	18.5	86	1.70	0.0225	86	104.5	0.177
A	15.00	1.37	20	0.112	37	86	1.70	0.0225	86	123	0.301
2A	30.00	2.74	40	0.225	74	86	1.70	0.0225	86	160	0.462
4A	60.00	5.49	80	0.450	148	86	1.70	0.0225	86	234	0.632
$C_E/4$	15.00	1.37	20	0.112	37	86	1.70	0.0056	86	123	0.301
$C_E/2$	15.00	1.37	20	0.112	37	86	1.70	0.0113	86	123	0.301
C_E	15.00	1.37	20	0.112	37	86	1.70	0.0225	86	123	0.301
$2C_E$	15.00	1.37	20	0.112	37	86	1.70	0.0450	86	123	0.301
$4C_E$	15.00	1.37	20	0.112	37	86	1.70	0.0900	86	123	0.301
$C_A/4$	15.00	1.37	20	0.112	37	86	0.42	0.0225	86	123	0.301
$C_A/2$	15.00	1.37	20	0.112	37	86	0.85	0.0225	86	123	0.301
C_A	15.00	1.37	20	0.112	37	86	1.70	0.0225	86	123	0.301
$2C_A$	15.00	1.37	20	0.112	37	85	3.40	0.0225	86	123	0.301
$4C_A$	15.00	1.37	20	0.112	37	83	6.80	0.0225	86	123	0.301
$8C_A$	15.00	1.37	20	0.112	37	75	13.60	0.0225	86	123	0.301
$16C_A$	15.00	1.37	20	0.112	37	64	27.18	0.0225	86	123	0.301
$24C_A$	15.00	1.37	20	0.112	37	60	33.89	0.0225	86	123	0.301
$32C_A$	15.00	1.37	20	0.112	37	54	42.83	0.0225	86	123	0.301
$36C_A$	15.00	1.37	20	0.112	37	52	47.12	0.0225	86	123	0.301

[a] EGMA: ethylene glycol dimethacrylate; DVB: divinylbenzene; BPO: benzoyl peroxyde; AG: acacia gum; SDS: sodium dodecylsulfate.
[b] V_{org}: organic (dispersed) phase volume; V_{aq}: aqueous (continuous) phase volume; $V_{total} = V_{org} + V_{aq}$; $\phi = V_{org}/V_{total}$. Volumes are measured at 25°C and before the addition of 2.5 l of same aqueous phase.

the volume is a function of two coordinates and the slope of the drop profile. Details of this apparatus are given by Faour et al.[21] and Boury et al. [22]. This tensiometer allows up to five measurements per second with an accuracy greater than 0.1 ± 10^{-3} N m^{-1}. For each measurement of the interfacial tension, the area and volume of the drop are recorded.

3.2.6. Size distribution determination

Since the gelation process is very fast, the distribution of the droplets diameters correspond to the distribution of the beads diameters. The beads diameters determination was carried out by using an optic microscope with a micrometer (magnification 150–750). This method was found to be more accurate than a laser counting method which gave roughly detailed distribution with two maxima.

Eqs. (15) and (23) were used; the beads number n is approximately 500 and m is the mass of these beads. The uncertainty of the beads diameters Δd is ± 2 μm.

4. Results and discussion

Mean diameter (number $\bar{d}^{nb}$, weight $\bar{d}^{w}$ or Sauter d_{32}) of a polymer beads distribution constitutes an important industrial parameter. For the direct prediction of the mean diameter, it would be necessary to take into account very complex breaking and coalescing phenomena which participates in the droplet formation. The maximum diameter of a distribution can be predicted by way of the theoretical relationships of Kolmogoroff and Taylor.

Afterwards, we will predict the maximum diameter values of a beads distribution in function of experimental parameters such as the interfacial tension and the kinematic or dynamic viscosity by the use of Kolmogoroff and Taylor's theories. The experimental relationship between the maximum diameter and Sauter mean diameter will also be established.

4.1. Choice of the phase volume fraction ϕ

$$\phi = \frac{V_d}{V_d + V_c}, \tag{25}$$

where V_d is the dispersed phase (organic phase) volume, V_c the continuous phase (aqueous solution of acacia gum and surfactant) volume.

Several authors have shown that d_{32} depends on the volume fraction by the relation:

$$d_{32} \propto f(\phi) d_{32}^0, \tag{26}$$

where d_{32}^0 is the d_{32} obtained when ϕ tends to 0. For Calderbank [23], Brown and Pitt [24], Mlynek and Resnick [25], Coulaloglou and Tavlarides [26], $f(\phi)$ is a linear function of ϕ

$$f(\phi) = a(1 + b\phi), \tag{27}$$

Table 2
Mean diameters $\bar{d}^{w}$, $\bar{d}^{nb}$ and d_{32} of beads versus the phase volume fraction ϕ

Series	A/4	A/2	A	2A	4A
ϕ [a]	0.099	0.177	0.301	0.462	0.632
$\bar{d}^{nb} \times 10^6(m)$	Aggregate	Aggregate	60	16	29
$\bar{d}^{w} \times 10^6(m)$	Aggregate	Aggregate	98.5	30	37
$d_{32} \times 10^6$(m)	Aggregate	Aggregate	92	27	39

[a] $\phi_d/(V_d + V_c)$ (V_d: dispersed phase volume, V_c: continuous phase volume before the addition of 2.5 l of the same phase). Volumes are measured at 25°C.

Table 3
Experimental parameters, mean diameters $\bar{d}^{nb}$, $\bar{d}^{w}$ and d_{32} and experimental maximum diameter $(d_{max})_{obs}$ for series C_E

Series[a]	$C_E/4$	$C_E/2$	C_E	$2C_E$	$4C_E$
C_{SDS}[b] $\times 10^4$ (mol/l)	2.26	4.55	9.07	18.14	36.28
$\sigma \times 10^3$ (N/m)	7.1	4.1	4.3	2.4	1.5
$(d_{max})_{obs} \times 10^6$ (m)	182	118	138	93	72
$d_{32} \times 10^6$(m)	116	74	92	44.5	28
$\bar{d}^{nb} \times 10^6$ (m)	63.5	50	60	25	13
$\bar{d}^{w} \times 10^6$ (m)	137	81	98.5	50	35.5
d_{32}/d_{max}	0.64	0.62	0.67	0.48	0.38
$\bar{d}^{w}/\bar{d}^{nb}$	2.15	1.62	1.65	2.01	2.65
N_{vi}[c] $\times 10^2$	1.61	2.64	2.38	3.89	5.59
$\Psi(N_{vi})$[c] $\times 10^3$	1.46	2.59	2.73	5.98	10.69

[a] For all series C_E:$C_{acacia} = 19.76$ g/l; $\rho_c = 980$ kg/m^3; $\mu_d = 5.32 \times 10^{-4}$ Pl; $\mu_c = 5.5 \times 10^{-4}$ Pl; $\nu_c = 5.61 \times 10^{-7}$ m^2/s; $\eta = 20.1 \times 10^{-6}$ m; Re = 88445; Ta (Taylor number, see Appendix B) = 14 050.

[b] C_{SDS}: sodium dodecyl sulfate concentration.

[c] $N_{vi} = \mu d/\sqrt{\rho_d \sigma d_{max}}$ with $\rho_d = 836$ kg m^{-3}; $\Psi(N_{vi}) = 1.077.(N_{vi})^{1.6}$ (see Appendix B).

where a is close to 0.06 and b lies between 3 and 6 according to those authors.

By fixing ϕ at 0.301, we maintain a proportional relationship between d_{32} and d_{32}^0. This volume fraction will be kept constant in experiments C_E and C_A. As it is shown in Table 2, when ϕ is smaller than 0.301, an agglomeration of the beads occurs and it is impossible to separate them out and consequently it is impossible to determine the droplet distribution at the gel point. The volume fraction was chosen in such a way that it may correspond to the higher important difference between the phases which yields non-agglomerated beads.

4.2. Determination of the turbulence microscale value η of Kolmogoroff

The turbulence microscale value is an important physical criteria because it allows to theoretically determine whether or not the viscosity plays a role in the phenomena of droplets splitting in the liquid suspension when the suspension is mechanically stirred.

The turbulence microscale η is calculated from Eq. (4):

$$\eta = \varepsilon^{-1/4} \nu_c^{3/4}, \tag{4}$$

where ε is the dissipated power by mixed mass unit, ν_c the kinematic viscosity (see Tables 3 and 4).

In order to determine ε, we measured the mechanic energy dissipated by the agitator at a speed of 5.5 revolutions/s for 20 min. This measurement was conducted by raising the temperature of 1 kg of water ($\Delta\theta$) in a calorimeter. The initial water temperature was close to room temperature (18°C), measured with an accuracy of 0.01°C.

Table 4
Experimental parameters, mean diameters $\bar{d}^{nb}$, $\bar{d}^{w}$ and d_{32} and experimental maximum diameter $(d_{max})_{obs}$ for series C_A

Series[a]	$C_A/4$	$C_A/2$	C_A	$2C_A$	$4C_A$	$8C_A$	$16C_A$	$24C_A$	$32C_A$	$36C_A$
C_{acacia}(g/l)	4.88	9.88	19.76	39.53	79.06	158.13	316.04	394.06	498.02	547.84
ρ_c (kg/m^3)	974	976	980	991	1002	1021	1057	1091	1121	1130
$\mu_c \times 10^3$ (Pl)	0.45	0.46	0.55	0.95	1.62	3.20	10.5	28.8	69.2	97.4
$\nu_c \times 10^7$ (m^2/s)	4.6	4.7	5.6	9.6	16.2	31.3	99.3	264.0	617.3	862.5
$\sigma \times 10^3$ (N/m)	7.3	5.8	4.3	3.6	3.6	3.6	3.6	3.6	3.6	3.6
$\eta \times 10^6$ (m)	17.4	17.7	20.1	30.0	44.6	73.0	173.5	361.3	683.1	877.9
Re[b]	106 726	104 635	88 445	51 779	30 550	15 837	4996	1880	804	575
Ta[b]	17 058	16 726	14 050	8134	4720	2458	818	293	136	90
p[c]	1.174	1.149	0.967	0.560	0.326	0.166	0.050	0.018	0.007	0.005
$f(p)$[c]	1.101	1.100	1.092	1.067	1.046	1.026	1.009	1.003	1.0014	1.0009
$(d_{max})_{obs} \times 10^6$ (m)	378	190	138	198	71	89	81	57	40.5	32.5
$d_{32} \times 10^6$ (m)	220	122	92	63	32	57	36.5	29	22	17
$\bar{d}^{nb} \times 10^6$ (m)	119	59	60	35.5	16	40	22	16	13.5	11
$\bar{d}^{w} \times 10^6$ (m)	256.5	141	98.5	89	45	62.5	43	35	26	20
d_{32}/d_{max}	0.58	0.64	0.67	0.32	0.47	0.77	0.63	0.52	0.69	0.70
$\bar{d}^{w}/\bar{d}^{nb}$	2.15	2.37	1.65	2.50	2.77	1.56	1.95	2.24	1.92	1.82
N_{vi}[d] $\times 10^2$	1.10	1.75	2.38	2.18	3.64	3.25	3.40	4.06	4.81	5.37
$\Psi(N_{vi})$[d] $\times 10^3$	0.80	1.66	2.73	2.36	5.36	4.48	4.83	6.39	8.38	10.03

[a] For all series C_A: $C_{SDS} = 9.07 \times 10^{-4}$ mol l^{-1}.

[b] Re is the Reynolds number; Ta is the Taylor number-see Appendix B.

[c] μ_d/μ_c with $\mu_d = 5.32 \times 10^{-4}$ Pl; $f(p) = (19p + 16)/(16p + 16)$.

[d] $N_{vi} = \mu_d/\sqrt{\rho_d \times \sigma \times d_{max}}$ with $\rho_d = 836$ kg m^{-3}; $\Psi(N_{vi}) = 1.077.\ (N_{vi})^{1.6}$ (see Appendix A).

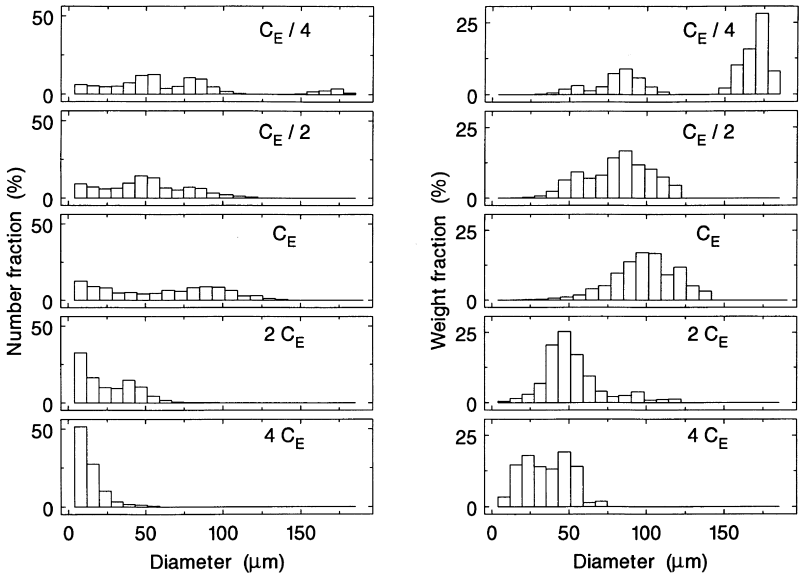

Fig. 4. Histograms of number and weight fraction of beads in experiments $C_E/4$ to 4 C_E.

The calorimeter had almost the same dimensions as our reactor.

The dissipated power is:

$$P = MC_p \frac{\Delta\theta}{\Delta t}, \tag{28}$$

where M is the mass of stirred liquid, $C_p = 4\,810\ \mathrm{J\,kg^{-1}\,K^{-1}}$, $\Delta\theta$ the temperature increase and t the time (s).

For 1 kg of water, P was found to be equal to 0.2 W. We consider that the same power per unit mass is dissipated in our aqueous suspensions experiments. The stirred water mass will be $\rho_w V$, where V is the volume taken to be equal to $(\pi l^2 e)/4$, where l is the length of the arc circle anchor-shaped stirrer of diameter D ($D = 0.095$ m), $l = 0.14$ m, e is the stirrer width, $e = 0.021$ m and $\rho_w = 10^3\ \mathrm{kg/m^3}$

$$\varepsilon = \frac{4P}{\pi l^2 e \rho_w} = 1.08\ \mathrm{W/kg}. \tag{29}$$

For a turbulent flow to be locally isotropic, D must be very large versus η and Re_T (the apparatus Reynolds number) must be high enough:

$$Re_T = \frac{ND^2}{\nu_c}. \tag{30}$$

N, D, ν_c keep their previous definitions. In general $Re_T > 10\,000$ is considered as an important high enough

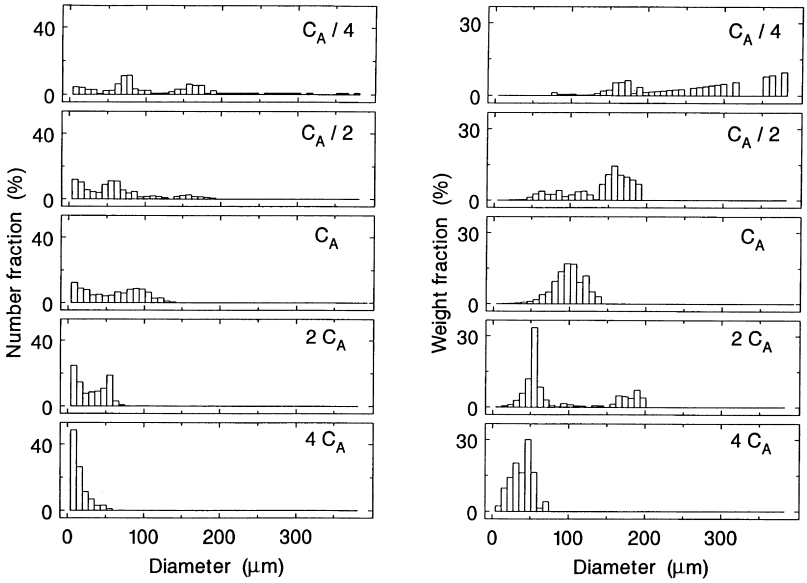

Fig. 5. Histograms of number and weight fraction of beads in experiments $C_A/4$ to 4 C_A.

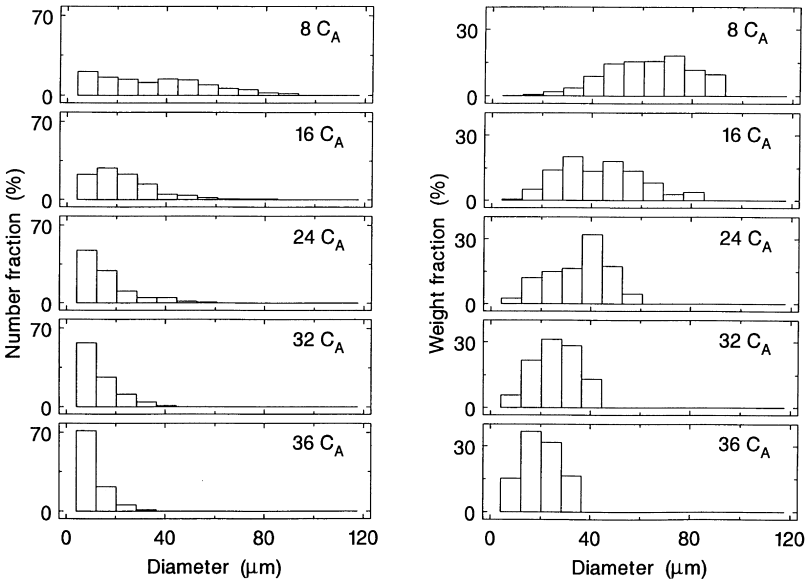

Fig. 6. Histograms of number and weight fraction of beads in experiments 8 C_A to 36 C_A.

value [27]. Tables 3 and 4 present the Kolmogoroff scale (η) and apparatus Re for all of the experiments.

4.3. Distribution of the bead diameters in C_E and C_A series

Figs. 4–6 represent the histograms of the number and weight fractions established according to Eqs. (15) and (16). As the gelation phenomenon is rather brief, the distribution of the polymer beads is identical to the monomer droplets distribution at the gelation time.

The C_E series were conducted at a constant kinematic viscosity of the continuous phase (ν_c) and varying interfacial tensions (σ). As the interfacial tension decreases a narrowing of the intervals of the beads diameters' values is observed. The smallest diameters found are close to 10 μm.

In the C_A series, the same pattern is observed, but in this case the interval narrowing is due to both an interfacial tension decrease and a kinematic and dynamic viscosity increase as it is reported in Table 4. However the 10 μm limit is also present in this case. It is important to observe that in each experiment $D \gg d \gg \eta$ is verified for the highest beads while for diameters close to 10 μm we have $D \gg \eta \gg d$, and this is true whether ν_c is constant (C_E series) or variable (C_A series).

Several authors [28–31] consider the droplets breakage as a random process of a big number of events. For a "mother" droplet of volume y, the "daughter" droplets of volume x are distributed around a mean value $\bar{x}$ according to a Gaussian distribution which does not correspond to our experiments as several maxima were found.

Only a few works have reported a bimodal distribution and none a multimodal distribution. Ward and Knudsen [29] explained the bimodality by a viscous erosion phenomenon of the droplets.

The stirring effect causes several small droplets to be extracted (pulled out) from the surface of much bigger droplets. Consequently, the bigger droplets diameter is only slightly diminished by the formation of tiny droplets. A similar explanation was advanced by Brown and Pitt [32].

If the Ward and Knudsen [29] mechanism could be applied to our values, the ratio $\bar{d}^w/\bar{d}^{nb}$ should increase as the viscous abrasion phenomenon increases. In fact, the mean diameter in mass $\bar{d}^w$ should be slightly affected by the appearance of very small beads whose total mass is very small. Conversely, the appearance of a large number of very small beads induces an important decrease of the mean diameter in number $\bar{d}^{nb}$ leading to a predictable increase of $\bar{d}^w/\bar{d}^{nb}$. Experimentally, the relation $\bar{d}^w/\bar{d}^{nb}$ may be considered to be constant, in spite of some experimental uncertainties due to the fact that it is difficult to accurately measure mean diameters and number fractions (see Tables 3 and 4). Thus, the Ward and Knudsen mechanism does not seem suitable to account for the distribution obtained in our experiments.

4.4. Maximum diameter in function of the interfacial tension with a constant viscosity of the continuous phase

The dynamic viscosity of the continuous phase (μ_c) was kept constant at 5.5×10^{-4} Poiseuille (Pl) by keeping a constant acacia gum concentration (C_E series). The interfacial tension measurement is obtained by the pendant drop method where σ values decrease in function of time until they reach an equilibrium value.

This phenomenon occurs when the solution contains a solubilized polymer. The adsorption process is based on the diffusion of surfactant molecules from the liquid bulk towards the interface and an energy barrier which corresponds to conformational changes as well as to the penetration of the interface.

In a mechanical stirred system, the diffusion can be

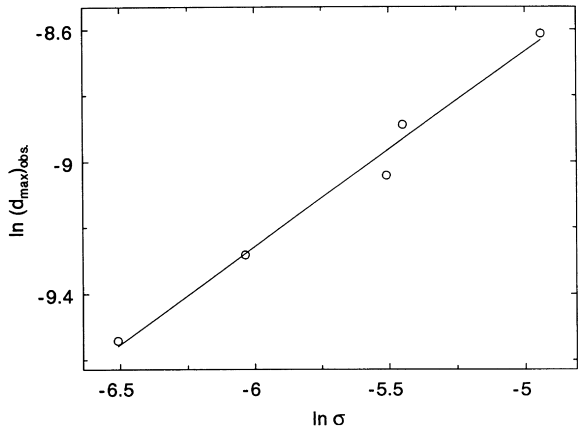

Fig. 7. Variation of $\ln (d_{max})_{obs}$ versus in σ for experiments C_E.

neglected and the concentration beneath the interface is that of the bulk. This is commonly used by biochemists while studying enzymatic activity at the interface [33,34]. From this fact we assimilate the interface tensions of our suspension polymerization to the adsorption kinetic equilibrium values obtained by the method of the pendant drop.

Eq. (10) shows that when $d \gg \eta$ the theoretical maximum diameter d_{max} depends only on ρ, σ, ε. In C_E series, ρ_c and ε were kept constant and Eq. (10) is reduced to:

$$d_{max} \propto \sigma^{3/5} \tag{31}$$

when $\ln(d_{max})_{obs}$ is plotted against $\ln \sigma$, the linear relationship (32) is obtained for C_E series (see Fig. 7)

$$\ln(d_{max})_{obs} = k_l + \alpha \ln \sigma. \tag{32}$$

We found from these data that $k_l = -5.71$ and $\alpha = +0.59$. α is close to the theoretical value of $+0.60$. Thus, the Kolmogoroff theory seems to be suitable to explain our results.

4.5. The effect of acacia gum concentration

Hydrosoluble polymers are widely used to reduce beads mean diameter, though their influence on viscosity has not yet been clearly defined, their main role being the reduction of coalescing.

In the C_A experiments, sodium dodecylsulfate concentration was kept constant (9.07×10^{-4} mol/l) and the acacia gum concentration was increased in a ratio of 1–112. As a consequence, the dynamic viscosity was increased in a ratio of 1–216 and the interfacial tension was reduced (see Table 4).

Comparing the values of $(d_{max})_{obs}$ to the values of η (see Table 4), three groups of beads diameter are found. These three groups are related to the following inequalities:

$$D \gg d_{max} \gg \eta, \tag{33}$$

$$D \gg d_{max} \sim \eta, \tag{34}$$

$$D \gg \eta \gg d_{max}. \tag{35}$$

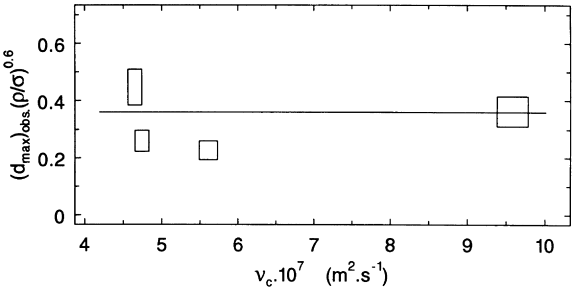

Fig. 8. Variation of $(d_{max})_{obs} \times (\rho_c/\sigma)^{3/5}$ versus ν_c for experiments C_A with $d_{max} \gg \eta$.

Let us now consider our results in the case of inequalities (33)–(35).

In the case where relation (33) is effective, the influence of kinematic viscosity ν_c should not be observed and the following relation can be applied:

$$d_{max} \propto (\sigma/\rho_c)^{3/5}. \tag{36}$$

Fig. 8 shows that $(d_{max})_{obs}\ (\rho_c/\sigma)^{3/5}$ is effectively constant within the experimental uncertainty.

According to the theory of isotropic and homogeneous turbulence, when $(d_{max})_{obs} \sim \eta$ is verified, there is no theoretical relationship between σ, ν_c and ε.

In contrast, under the conditions of relation (35), the viscosity may influence the droplets diameter according to the first hypothesis of Kolmogoroff [11,12].

Therefore the relation (37) (see Appendix A) should be applied:

$$d_{max} \propto (\nu_c \sigma/\rho_c)^{1/3}. \tag{37}$$

Fig. 9 shows that there is a linear relationship between $\ln(d_{max})_{obs}$ and $\ln \nu_c\sigma/\rho_c$, but with a power of -0.42 instead of 1/3. Also it is seen that whenever $\nu_c\sigma/\rho_c$ increases $(d_{max})_{obs}$ decreases, which is contrary to the theoretical predictions where $(d_{max})_{obs}$ should increase as $\nu_c\sigma/\rho_c$ increases, the proportionality coefficients being positive.

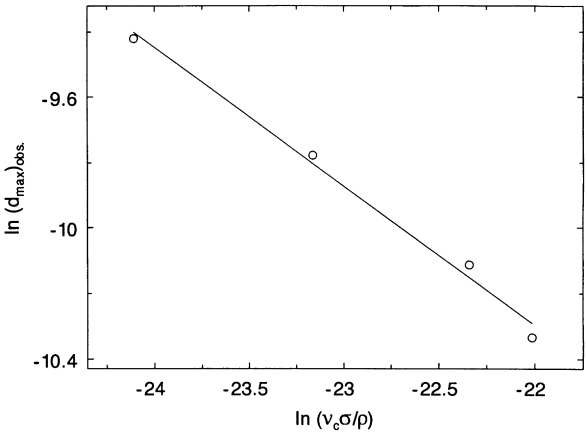

Fig. 9. Variation of $\ln (d_{max})_{obs}$ versus $\ln \nu_c\sigma/\rho_c$ for experiments C_A with $\eta \gg d_{max}$.

In several experimental studies, the dynamic viscosity parameter of the continuous phase μ_c is taken into account by power relations of the following type:

$$d_{obs}/D = k\sigma^s \mu_c^m \rho_c^\theta. \quad (38)$$

For Rodger [35]: $s = 0.36$, $m = -0.2$ and $\theta = 0.36$, Sprow [7]: $s = 1$, $m = -0.5$ and $\theta = -1.5$, Lazo [36]: $s = 0.4$ and $m = 0.056$ (θ not given), Hopff [37]: $s = 0.9$ and $m = 1$ (θ not given). These dispersed data are not useful because there is no mention of the d_{obs} values compared to η. To our knowledge, the validity of relation (37) has never been confirmed. We consider that the viscosity is the determining factor on the droplets diameter instead of the inertial breakage. Thus, we must consider the existence of a different droplet breakage mechanism when $\eta \gg d_{max}$.

In order to verify $\eta \gg d_{max}$ we had to greatly increase the viscosity, thus Taylor's number and Reynold's number were decreased (see Table 4).

Therefore, the issue of the laminar or turbulent nature of our flow raises here. In the case of a fluid flowing across two concentric cylinders, where one of them is in rotational movement, Taylor showed that a laminar domain is established with presence of vortices whenever $41.3 < Ta < 400$ [38] (see Appendix B). Although the stirring in our reactor induces a different flow than in the previous cases (33) and (34), we assume a laminar flow in the experiments where the relation $\eta \gg d_{max}$ is verified (see Table 4). Thus, relation (14) has to be considered in this case

$$d_{max} = \frac{\sigma}{2G\mu_c\left[\dfrac{19p+16}{16p+16}\right]}. \quad (14)$$

Fig. 10 shows that there is really a linear relationship by plotting $(d_{max})_{obs}$ versus $\sigma/[\mu_c(19p + 16)/(16p + 16)]$. Thus, the Taylor's theory seems to be suitable to explain our results.

4.6. Relation between the maximum and mean diameters

In many cases, the proportional relation (39) is generally admitted between $(d_{max})_{obs}$ and d_{32}.

$$d_{32} = k_2(d_{max})_{obs}. \quad (39)$$

Values of the ratio $d_{32}/(d_{max})_{obs}$ found in the literature are equal to 0.38, 0.50, 0.50 and 0.70 according to Sprow [7], Van Heuven [39], Mc Mamaney [40] and Brown and Pitt [41], respectively. The value of the relation $d_{32}/(d_{max})_{obs}$ strongly depends on the reactor design and the operating conditions as it is seen from the dispersed values listed for k_2. In our reactor, the mean of 14 values of k_2 is equal to 0.58.

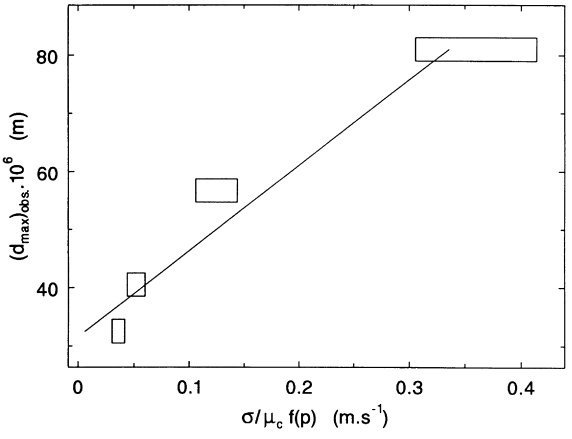

Fig. 10. Variation of $(d_{max})_{obs}$ versus σ/μ_c $f(p)$ for experiments C_A with $\eta \gg d_{max}$; $f(p) = (19p + 16)/(16p + 16)$ and $p = \mu_d/\mu_c$.

5. Conclusion

From the study of a suspension polymerization in toluene of EGDMA–DVB, we have deduced two mechanisms for the breakage of the droplets of monomers.

Comparing the experimental maximum diameter $(d_{max})_{obs}$ of the polymer beads to the Kolmogoroff's scale of turbulence η, we can assume that:

(i) When $(d_{max})_{obs} \gg \eta$, the experimental results lead to a dependence of $(d_{max})_{obs}$ as a function of $(\sigma/\rho_c)^{0.59}$. This exponent is very close to the theoretical exponent (3/5) appearing in the inertial breakage theory of Kolmogoroff. The droplet splitting can therefore be described by an inertial breakage.

(ii) When $(d_{max})_{obs} \ll \eta$, the experimental data show that $(d_{max})_{obs}$ obeys to $(d_{max})_{obs} = \sigma/[\mu_c(19p + 16)/(16p + 16)]$, ($p = \mu_d/\mu_c$, μ_d and μ_c are the dynamic viscosity of the dispersed and continuous phase, respectively). This relation corresponds to the viscous shear abrasion theory of Taylor. The droplet splitting can therefore be described by a viscous shearing.

Appendix A. Theoretical maximum diameter and fixed Weber number We_T

Weber number We is the ratio of kinetic energy, $1/2\ m\ v^2$, to the interface tension energy σd^2 and represents the energy required to cause a break up of a droplet in a turbulent dispersion. When we consider the particular maximum diameter d_{max}, Weber number is called the critical Weber number, We_{crit} and it can be expressed as follows [14]:

$$We_{crit} = C(1 + \Psi(N_{vi})), \quad (A.1)$$

where C is a dimensionless constant. N_{vi} the viscosity number which accounts for the effect of the viscosity of the dispersed droplet and it can be expressed as $\mu_d/\sqrt{\rho_d \sigma d}$, where μ_d, ρ_d, σ and d are the dispersed phase dynamic viscosity, dispersed phase density, interfacial tension, and size of the considered droplet, respectively. $\Psi(N_{vi})$ is a function of N_{vi} which has been formulated as [42]: $\Psi(N_{vi}) = 1.077(N_{vi})^{1.6}$.

In all of our experiments, $\Psi(N_{vi}) \ll 1$ (see Tables 3 and

4), in consequence the critical Weber number is a constant which can be expressed for an isotropic turbulence by [14]:

$$We_{crit} \propto \frac{\nu^2 \rho_c d_{max}}{\sigma}, \quad (A.2)$$

ν^2 is the mean square of the turbulent flow.

In the case where $d_{max} \gg \eta$ we have:

$$\nu^2 \propto (\varepsilon d_{max})^{2/3}. \quad (A.3)$$

The Weber critical number We_{crit} becomes:

$$We_{crit} \propto \left(\frac{\rho_c}{\sigma}\right)\varepsilon^{2/3} d_{max}^{5/3}. \quad (A.4)$$

In Eq. (A.4) We_{crit} can be replaced by the Weber number of the apparatus We_T [43]:where

$$We_T = \frac{N^2 D^3 \rho_c}{\sigma} \quad (A.5)$$

$$\varepsilon = K N^3 D^2, \quad (A.6)$$

where N is the stirrer rotation speed, K the dimensionless constant depending on the reactor design, D the stirrer diameter.

When D and N are kept constant:

$$d_{max} \propto \left(\frac{\sigma}{\rho_c}\right)^{3/5}. \quad (36)$$

In the case where $d_{max} \ll \eta$:

$$\nu^2 \propto \left(\frac{\varepsilon}{\nu_c}\right) d_{max}^2. \quad (A.7)$$

Eq. (36) allows to obtain:

$$We_{crit} \propto \left(\frac{\varepsilon}{\nu_c}\right)\left(\frac{\rho_c}{\sigma}\right) d_{max}^3, \quad (A.8)$$

$$We_T \propto \left(\frac{\varepsilon}{\nu_c}\right)\left(\frac{\rho_c}{\sigma}\right) d_{max}^3. \quad (A.9)$$

When D and N are maintained constant:

$$d_{max} \propto \left(\frac{\nu_c \sigma}{\rho_c}\right)^{1/3}. \quad (37)$$

Appendix B. The Taylor number

The Taylor number (Ta) allows to characterize the conditions in which a liquid flowing around two concentric cylinders becomes unstable [38]. It is expressed in the following form:

$$Ta = \frac{u\delta}{\nu}\sqrt{\frac{\delta}{r_i}}, \quad (B.1)$$

where u is the velocity of the flow, ν the kinematic viscosity of the flow. $\delta = R - r_i$, δ denotes the gap width, R is the highest cylinder radius r_i the inner cylinder radius. When $Ta < 41.3$: the flow becomes a laminar flow; $41.3 < Ta < 400$: the flow is a laminar flow with vortices; $Ta > 400$: the flow is a turbulent flow.

References

[1] Yang CM, Hamann HC. J Appl Polym Sci 1980;25:2555.
[2] Blondeau D, Bigan M, Despres P. React Funct Polym 1995;27:163.
[3] Lee KY, Kim KS, Moon YU, Jac-sup S. Hongop Hwahak 1995;6:1180.
[4] Sakado H, Kida S. Japan Pat. 87-2095 870108, Chemical Abstracts, 109: 231 745.
[5] Rodriguez F. Principle of polymer system, 3. New York: Hemisphere Publishing, 1989 p. 133.
[6] Odian G. Principle of polymerization, 3. New York: Wiley, 1991 p. 302.
[7] Sprow FB. Chem Engng Sci 1967;22:435.
[8] Nass LI, Heiberger CA, editors. 2. Encyclopedia of PVC, 1. New York: Wiley, 1985. pp. 109.
[9] Kirk RE, Othmer DF, editors. 3. Encyclopedia of chemical technology, 1. New York: Wiley, 1978. pp. 453.
[10] Frish U. Turbulence: the legacy of A.N. Kolmogoroff, New York: Cambridge University Press, 1995 p. 27.
[11] Kolmogoroff AN. Doklady Akad Nauk SSSR 1949;66:825.
[12] Schiestel R. Modélisation et simulation des écoulements turbulents, Paris: Hermés, 1993 p. 27.
[13] Lesieur M. La turbulence, Grenoble: Presse Universitaire de Grenoble, 1994 p. 90.
[14] Hinze JO. AIChE J 1955;1:289.
[15] Leng DE, Quarderer GJ. Chem Engng Commun 1982;14:177.
[16] Taylor GI. Proc Roy Soc Lond 1932;138A:41.
[17] Taylor GI. Proc Roy Soc Lond 1934;146A:501.
[18] Taylor GI. Proc Roy Soc Lond 1954;226A:34.
[19] Karam HJ, Bellinger JC. Ind Engng Chem Fund 1968;7:576.
[20] Holmes DBR, Von Chen RM, Deiker JA. Chem Engng Sci 1964;19:201.
[21] Faour G, Grimaldi M, Richou J, Bois A. J Colloid Interf Sci 1996;181:385.
[22] Boury F, Ivanova T, Panaïtov I, Proust JE, Bois A, Richou J. Langmuir 1995;11:1636.
[23] Calderbank PH. Trans Inst Chem Engng 1958;36:43.
[24] Brown DE, Pitt K. Proc Chemeca (Melbourne, Sydney) 1970;70:83.
[25] Mlynek Y, Resnick W. AIChE J 1972;18:122.
[26] Coulaloglou CA, Tavlarides LL. AIChE J 1976;22:289.
[27] Rushton JH, Costich EW, Everett HJ. Chem Engng Progr 1950;46:395.
[28] Bates RL, Fondy PL, Corpstein RR. Ind Engng Chem Progr Design Develop 1963;2:310.
[29] Ward JP, Knudsen JG. AIChE J 1967;13:356.
[30] Chen HT, Middeman S. AIChE J 1967;13:989.
[31] Calabrese RV, Wang CY, Bryner NP. AIChE J 1986;32:677.
[32] Brown DE, Pitt K. Chem Engng Sci 1972;27:557.
[33] Verger R, De Hass GH. Annu Rev Biophys Bioengng 1976;5:77.
[34] Verger R. Methods Enzymol 1980;64:340.
[35] Rodger WA, Trice VG, Rushton JH. Chem Engng Progr 1956;52:515.
[36] Lazo M, Steiner L, Hartland S. Chem Eng Sci 1987;42:2437.
[37] Hopff H, Lüssi H, Gerspacher P. Makromol Chem 1964;78:37.
[38] Schlichting H. Boundary-layer theory, New York: McGraw-Hill, 1961 p. 425.
[39] Van Heven JW, Hoevenaar JC. Proc. 4th European Symp. React. Engng, Burssel 1968;:217.
[40] Mc Mamaney WJ. Chem Engng Sci 1974;34:432.
[41] Brown DE, Pitt K. Chem Engng Sci 1974;29:345.
[42] Cohen RD. Int J Multiphase Flow 1994;20:211.
[43] Shinnar R, Church JM. Ind Engng Chem 1960;52:253.